NUMERICAL INVESTIGATION OF A JET IN GROUND EFFECT USING THE FORTIFIED NAVIER-STOKES SCHEME

William R. Van Dalsem and Joseph L. Steger
NASA Ames Research Center, Moffett Field, CA.

SUMMARY

One of the flows inherent in VSTOL operations, the jet in ground effect with a crossflow, is studied using the Fortified Navier-Stokes (FNS) scheme. Through comparison of the simulation results and the experimental data, and through the variation of the flow parameters (in the simulation) a number of interesting characteristics of the flow have been observed. For example, it appears that the forward penetration of the ground vortex is a strong inverse function of the level of mixing in the ground vortex. Also, an effort has been made to isolate issues which require additional work in order to improve the numerical simulation of the jet in ground effect flow. The FNS approach simplifies the simulation of a single jet in ground effect, but will be even more effective in applications to more complex topologies.

FLOW TOPOLOGY

Most VSTOL aircraft use propulsive thrust to supply control and lift forces near a landing surface at low forward speeds. In many cases, these forces are created by a jet issuing at an angle to the line of flight and impinging on a solid surface. Therefore, the jet in ground effect flow, shown in figure 1a, has been the subject of considerable experimental work (e.g., refs. 1-6). This flow contains many of the basic fluid dynamics phenomena which are important in VSTOL flows, yet does not involve complex geometry or grid generation. Therefore, its study is a good "first step" in the application of CFD to the VSTOL area. Specifically, in the present work an effort has been made to computationally simulate the experimental setup of Stewart, Kuhn, and Walters (refs. 1-2).

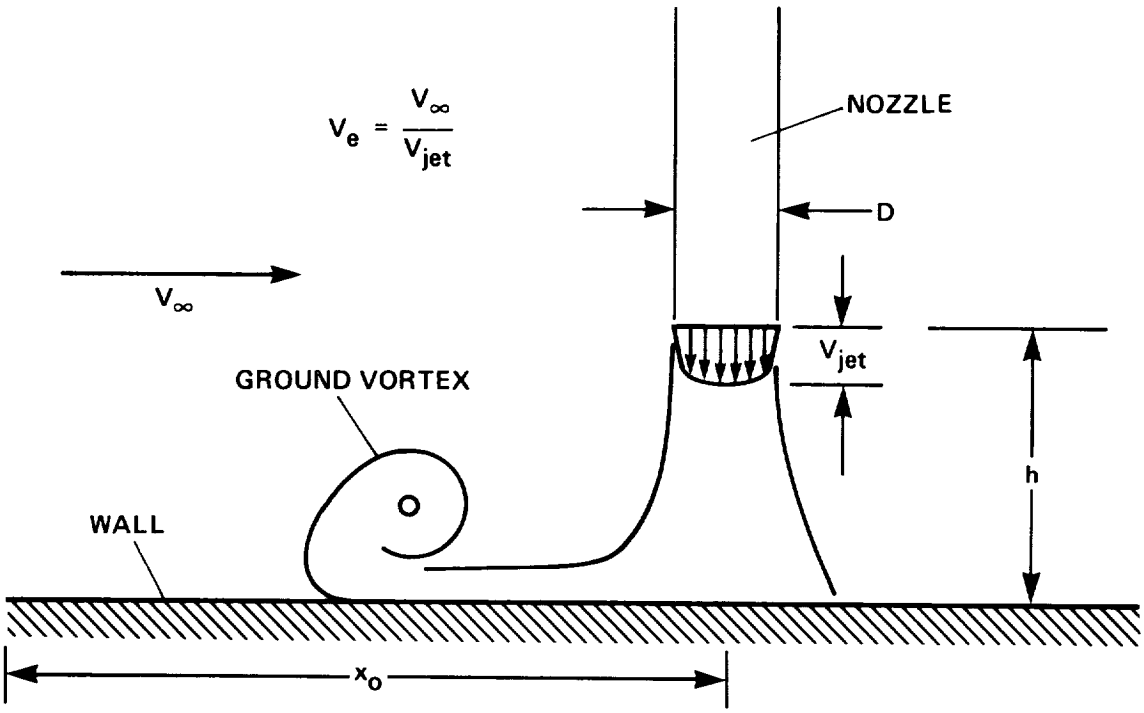

Figure 1a.- Jet in ground effect with a crossflow.

NUMERICAL APPROACH AND GRID TOPOLOGY

This flow was simulated by solving the Reynolds-averaged, Navier-Stokes equations using an implicit, partially flux-split, two-factor algorithm (ref. 7). To account for the viscous stresses normal to the wall (ζ-direction) and normal to the nozzle body (ξ-direction) the thin-layer viscous terms in both these directions have been included. At this point, the viscous cross terms have not been included as they should be important only at isolated corners of the grid. Also, only the ζ direction viscous terms are treated implicitly, which significantly simplifies the algorithm.

The FNS scheme (refs. 8-10) was originally envisioned as a simple way to couple various numerical algorithms and formulations. For example, in references 8-9, three-dimensional boundary-layer and Euler/Navier-Stokes algorithms are coupled using the FNS scheme. It was shown that a significant improvement in the performance (i.e., computer time required to obtain a solution of a given accuracy) of the Navier-Stokes algorithm could be obtained. However, it has since been recognized that the FNS scheme can also be used to patch, overset, or enrich grid systems. Furthermore, it is useful in imposing conditions within a computational domain. These last two capabilities are useful in simplifying the grid-interfacing and generation problems. It is the ability to impose conditions within the computational domain that is used in the work presented here.

In the FNS scheme a simple numerically stabilizing source term is implicitly added to the numerical algorithm in any region in which a "solution" is known from another predictive scheme. For example, the FNS scheme is added to the partially flux-split, two-factor algorithm by including the underlined terms

$$\begin{aligned}
&\left[I + \underline{h\chi I} + h\delta_\xi^b(\widehat{A}^+)^n + h\delta_\zeta \widehat{C}^n - hRe^{-1}\bar{\delta}_\zeta J^{-1}\widehat{M}^n J - D_i|_\zeta\right] \\
&\times \left(I + \underline{h\chi I}\right)^{-1} \\
&\times \left[I + \underline{h\chi I} + h\delta_\xi^f(\widehat{A}^-)^n + h\delta_\eta \widehat{B}^n - D_i|_\eta\right] \Delta\widehat{Q}^n = \\
&- \Delta t\{\delta_\xi^b[(\widehat{F}^+)^n - \widehat{F}_\infty^+] + \delta_\xi^f[(\widehat{F}^-)^n - \widehat{F}_\infty^-] + \delta_\eta(\widehat{G}^n - \widehat{G}_\infty) \\
&+ \delta_\zeta(\widehat{H}^n - \widehat{H}_\infty) - Re^{-1}\bar{\delta}_\xi(\widehat{S}_\xi^n - \widehat{S}_{\xi\infty}) - Re^{-1}\bar{\delta}_\zeta(\widehat{S}_\zeta^n - \widehat{S}_{\zeta\infty})\} \\
&- (D_e|_\eta + D_e|_\zeta)(\widehat{Q}^n - \widehat{Q}_\infty) + \underline{h\chi(\widehat{Q}_f - \widehat{Q}^n)}
\end{aligned}$$

where $\widehat{Q}$ is the solution vector and $\widehat{Q}_f$ is the forcing solution vector obtained from another source. (The reader is referred to ref. 7 for a detailed description of the base algorithm.) When $\chi = 0$, the original algorithm is recovered. However, as χ becomes very large, the algorithm reduces to

$$h\chi\Delta\widehat{Q}^n = h\chi(\widehat{Q}_f - \widehat{Q}^n)$$

or simply

$$\widehat{Q}^{n+1} = \widehat{Q}_f$$

Therefore, in any region where an accurate (or known) solution can be obtained, it can be built into the Navier-Stokes scheme. For example, $\widehat{Q}_f$ could be obtained from a specialized solver (e.g., a boundary-layer algorithm (refs. 8 and 9)), another grid zone (useful for grid patching or overlapping), or a known condition (such as at the face of an actuator disk). It is important to emphasize that χ is only a blending or switching function, and that it is not a "fudge factor." In regions where it is not desired to force the Navier-Stokes algorithm χ is simply set to zero, whereas χ is set to some large value (e.g., 1000 or 10,000) in regions where and when forcing is desired.

An important attribute of the FNS scheme is that in regions where the solution vector $\widehat{Q}_f$ is specified and χ is large, a large diagonal term is added to the implicit matrix operators, which increases the diagonal dominance of the matrices and (as shown in ref. 8) improves the convergence rate of the algorithm. From this point of view, it could be said that the solution vector $\widehat{Q}_f$ is used to condition the inversion matrices. A great deal of flexibility is available as χ can be a function of ξ, η, ζ, $\widehat{Q}$, $\widehat{Q}_f$, time, or even a positive definite operator. For example, in the grid oversetting application, in which multiple solutions are available in the overlap regions, χ could be varied to produce a smooth blending of the solutions.

In the current work the FNS scheme is used only to simplify the grid topology needed to simulate the nozzle/jet/ground geometry shown in figure 1b. A cylindrical coordinate system is used because it allows a natural clustering of the points to the shear layers created by both the nozzle body and the jet. A disadvantage of the cylindrical

coordinate system is that it introduces an axis boundary condition at the center of the jet. Using the FNS capability, the nozzle body no-slip conditions are imposed within the grid along a portion of a constant ξ plane. Similarly, the jet conditions are imposed on a subset of a constant ζ plane. The ability to insert conditions internal to the boundaries of the computational domain (e.g., the nozzle body and face) allows this geometry to be easily modeled with a single, simple, stretched-cylindrical-coordinate system. Without the FNS approach, multiple grid zones would have been required.

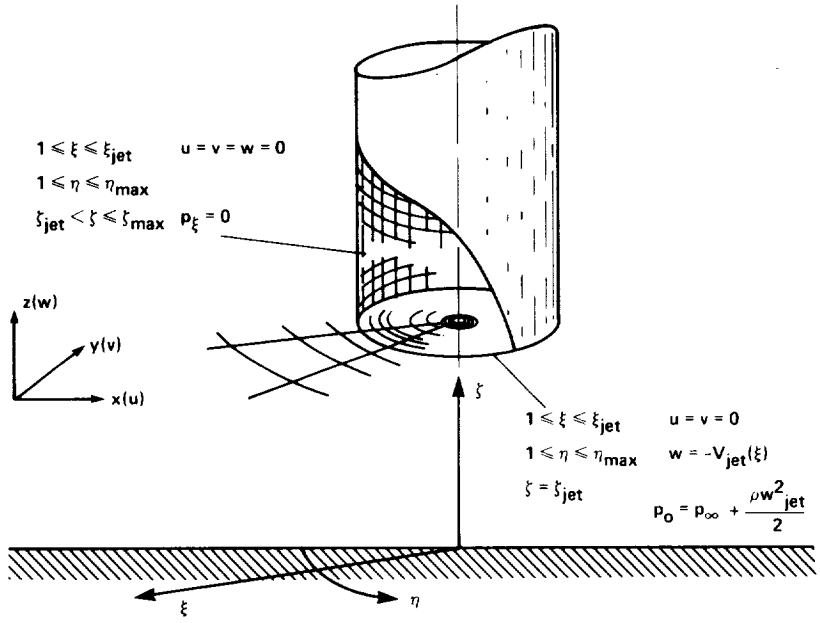

Figure 1b.- Jet and nozzle treatment.

RESULTS

The jet-in-ground-effect flow for $V_e = 0.223$, $h/D = 3$, and $x_0/D = 30$ was studied extensively. The experimentally measured jet profile was inserted at the nozzle exit. Also, in general it was assumed that the boundary-layer transitions to turbulent very near the leading edge of the plate.

Grid Refinement

Initially, the flow was computed assuming that the entire flow was completely turbulent using the Baldwin-Lomax turbulence model (ref. 11), including the modifications suggested by Schiff and Degani (ref. 12). The simulated oil-flow pattern presented in figure 2 shows jet impingement and the characteristic horseshoe vortex pattern observed experimentally. However, comparison with the experimental C_p distribution (measured along the jet centerline) shown in figure 3a indicates that the C_p minimum (corresponding to the location of the ground vortex) is too far forward. These computations were first performed on a 49 (radial) x 35 (circumferential) x 49 (normal to the

wall) grid. After studying the flow as resolved on this grid, it appeared that the grid was not fine enough in the radial direction to resolve the radial gradients in the ground-vortex region. Therefore, the grid was increased from 49 x 35 x 49 (84,035 points) to 82 x 35 x 49 (140,063 points), with most of the additional points clustered to the ground-vortex region. As shown in figure 3a, grid refinement did not affect the ground-vortex location, but did allow the resolution of higher gradients within the ground vortex. It is somewhat reassuring that the pressure gradients within the ground vortex resolved on the finer mesh are roughly the same as those observed experimentally.

Ground-Vortex Upstream Penetration and Turbulence Modeling

This initial simulation captured all the basic flow phenomena (specifically, the jet impingement and the ground vortex), but failed to accurately predict the location of the ground vortex. In an attempt to understand the ground-vortex flow a number of the flow field parameters were varied. For example, the initial jet profile was varied from that observed experimentally to an ideal slug flow. Also, the Reynolds number of the flow was varied over two-orders of magnitude. Various far-field boundary conditions were also studied. In general, it was found that the ground-vortex location was relatively insensitive to all of these variations.

It was observed that the ground-vortex location is very sensitive to the level of mixing in the boundary layer produced by the jet which moves upstream and forms the ground vortex. For example, if it is assumed that the flow is entirely laminar, then the ground vortex moves far upstream (figs. 3b and 4a). Similar results are obtained when the oncoming flow is retained as turbulent and only the wall flow moving upstream is assumed laminar (i.e., the ground-vortex region). Conversely, if it is assumed that the turbulence intensity in the boundary layer formed by the jet is underpredicted and should be greater, then the ground vortex moves back past the location that was observed experimentally (figs. 3b and 4b). Specifically, if the turbulent viscosity in the boundary layer emanating from the jet impingement point and moving upstream is increased by a factor of 10, the ground vortex moves back and sits just in front of the jet. A further increase of the turbulent viscosity in the jet footprint does not significantly change the ground-vortex location (fig. 3c). It appears that this reduced sensitivity to the turbulence intensity (at high turbulence levels) is due to the fact that the ground vortex is already "sitting" on the front of the jet, and further downstream motion is not possible.

From the numerical experimentation just described, it appears that the extent of forward penetration of the ground vortex is a strong function of the level of turbulent mixing in the ground-vortex region. In particular, to achieve agreement with the experimentally observed ground-vortex location it is necessary to increase the amount of turbulent mixing (predicted by the Baldwin-Lomax turbulence model) in the ground vortex. At this point we returned to experimental observations for guidance.

Kuhn, DelFrate, and Eshleman (ref. 13) prepared a video recording of a recent jet-in-ground-effect study made at the NASA Ames/Dryden Research Center Flow Visualization Facility. From viewing this video tape it is clear that there is intense large scale mixing in the ground-vortex region. Furthermore, some of this mixing is of such a large scale that it appears that we should be resolving it, while we must still supply an appropriate model for the turbulent mixing below our grid resolution.

Because the Baldwin-Lomax model was developed for thin boundary-layer flows, it is very likely that it is not adequate for this ground-vortex region.

The Baldwin-Lomax model represents one of two basic approaches to turbulence modeling. This model assumes that none of the turbulent mixing is resolved, and attempts to model all effects of turbulence. Another approach is to attempt to resolve the larger turbulent structures and only model the small scale turbulent mixing using a Sub-Grid-Scale (SGS) model. The advantage of this approach is that there is reason to believe that models for the small-scale turbulent mixing may be more universal. This concept has a long history. One of the first references to this concept appeared in 1932 and is due to G. I. Taylor (ref. 14). The concept has since been used in weather prediction (e.g., Smagorinsky's work (ref. 15)) and Large-Eddy-Simulation (e.g., ref. 16), and has recently been applied to the jet-upwash problem by, for example, Childs and Nixon (ref. 17), and Rizk (ref. 18).

One of the simpler SGS models, used for example by Childs and Nixon (ref. 17), is:

$$\mu_{SGS} \doteq c_1 \Delta z^2 |w|$$

where Δz is a representative grid-spacing length scale. This model is in contrast to the general character of the Baldwin-Lomax model which we can roughly represent in the following form:

$$\mu_{BL-INNER} \doteq c_2 z^2 |w|$$
$$\mu_{BL-OUTER} \doteq c_3 z_{max}^2 |w|_{max} F_{KLEB}$$

where z is the distance normal from the surface and the max subscript indicates the values of z and $|w|$ at which $z|w|[1 - exp(-y^+/A^+)]$ is maximum (c_1, c_2, and c_3 are simple numerical constants). Among the interesting differences between these models is that as the grid is refined (and more of the turbulent mixing is captured) the SGS model inserts less eddy viscosity, while the Baldwin-Lomax model is not grid dependent and is inconsistent in the limit of a very fine mesh.

If both these models are applied to the ground-vortex flow (figs. 5a and b) drastically different eddy viscosity levels are predicted. It appears that the Baldwin-Lomax model predicts high turbulence levels near the wall, but misses entirely the outer vortex region. On the other hand, the SGS model does not predict the correct near-wall behavior, but seems to model the large amount of turbulent mixing in the ground-vortex region which is observed in the video tapes of the experiment. This must be accounted for if the numerical simulation is to predict the ground-vortex location observed experimentally.

One approach is to use the SGS model throughout the bulk of the flow, but to return to the Baldwin-Lomax model near the wall. This results in the C_p distribution denoted as "modified SGS" in figure 5c. In this case, without ad hoc variation of the turbulence coefficients one obtains the ground vortex in roughly the correct location. Unfortunately, the shape of the C_p distribution is not correct. Indicating that overall we may have made some progress, but that more work is required.

It is apparent that the turbulent mixing in the ground-vortex region strongly influences the ground-vortex location; however, it is not clear what the mechanism

is that makes the ground-vortex flow so unsteady and results in the large amount of mixing. Some of the recent flow visualizations of Billet (ref. 19) indicate that a train of vortices is created by the shearing action between the jet and the freestream and that these vortices move up into the ground vortex and then "burst." Also, the recent work of Kuhn, DelFrate, and Eshleman (ref. 13) indicated that the resulting flow is not a strong function of the turbulent levels of the jet. These two points indicate that the large mixing in the ground vortex is due to unsteadiness inherent in the flow, and is not due to variations in the jet. On the other hand, recent work by Rizk (ref. 18) indicates that axisymmetric or azimuthal pulsing of the jet can create much different spreading rates in the resulting upwash flows. Perhaps, this flow is "self-exciting" and jet unsteadiness is not required to generate the large mixing, but may enhance it. For example, the moderate variations in the forward extent of the ground vortex indicated in figure 2 of the paper in this proceedings by Kuhn, DelFrate, and Eshleman may be due in part to variations in the nature of the jet flow.

Observed Jet Deformation

The front and side views of the traces of the particles released from the jet face, shown in figures 6 and 9a respectively, indicate a flow feature which may be difficult to observe experimentally. From the front view it appears that the jet is expanding rapidly as it leaves the nozzle, while the side view shows that the jet is contracting. This follows if one considers the pressures induced on the surface of the jet by the freestream flow (similar to those induced on a cylinder in crossflow). It appears that the high pressures on the front and back of the jet, and the low pressures on the sides of the jet are acting to deform the jet into an oval with the major axis normal to the freestream. Then shear stresses act to tear the ends off this oval (fig. 7), and create the swirling flow structure behind the jet.

From these observations it appears that a jet of elliptical cross-section with the major axis aligned with the flow would be more resistant to the break-up caused by the interaction with the freestream. Furthermore, such a jet nozzle would be more streamline than a round jet nozzle. Indeed, the jet nozzles on the Harrier aircraft are roughly of elliptical cross-section with the major axis parallel with the direction of forward flight.

h/D Variation

This flow was also computed at an $h/D = 6$. From the traces of particles released from the nozzle face (fig. 8), it appears that under these conditions the jet impinges upon the wall, but that a ground vortex does not form. According to reference 1, jet impingement may begin at $h/D = 10$ (for this V_e), and definitely occurs by $h/D = 6$; while the ground vortex does not form until $h/D = 4$. Hence, the numerical results at $h/D = 3$ (jet impingement and ground-vortex formation) and at $h/D = 6$ (jet impingement and no ground-vortex formation) correlate with experimental observation.

Nozzle vs. Actuator Disk Jet Sources

The difference between the jet issuing from a nozzle (a mass source) typically studied experimentally and the jet created by a rotor or jet engine (which are momentum but not mass sources) was also studied. In the latter case, nearby flow is entrained into the jet, which can be modeled as an actuator disk. Figures 9a-b show the particle

traces created by these two types of flow. Overall the flows are fairly similar, but the differences are great enough that caution should be used in studying one flow to understand the other. For example, in the nozzle case the forward extent of the ground vortex is greater, the vortex is flatter, and there is less defined structure behind the jet than in the actuator disk case.

CONCLUSIONS

A Fortified Navier-Stokes (FNS) algorithm has been applied to the jet-in-ground-effect flow and the results have been compared and contrasted with experimental data. From this work it appears that:

1. The FNS approach simplifies the simulation of the single jet in ground effect, but will be even more critical for the more complex topologies.
2. At least 140,000 points are required to resolve the numerous high-gradient regions (e.g., ground boundary layer, jet/freestream shear layer, and the ground vortex) in this flow.
3. The forward penetration of the ground vortex is a strong function of the turbulent mixing in the ground-vortex region, and more effort is required to either resolve or model the mixing in this region.
4. The numerical simulation predicts the characteristic jet footprint observed experimentally, and allows additional insight into the deformation of the jet by the freestream.
5. By varying h/D in the numerical simulation, it is possible to correlate with the experimental observations on jet impingement and ground-vortex formation as a function of h/D.
6. Nozzle jet flows (mass/momentum source) may produce a ground vortex which penetrates farther upstream and is of a smaller vertical extent than the ground vortex created by a jet engine installation (momentum source).

REFERENCES

1. Stewart, V. R.; Kuhn, R. E.; and Walters, M. M.: Characteristics of the Ground Vortex Developed by Various V/STOL Jets at Forward Speed. AIAA Paper No. 83-2494, Oct., 1983.
2. Stewart, V. R.; and Kuhn, R. E.: A Method for Estimating the Propulsion Induced Aerodynamic Characteristics of STOL Aircraft in Ground Effect. NADC 80226-60, Aug., 1983.
3. Colin, P. E.; and Olivari, D.: The Impingement of a Circular Jet Normal to a Flat Surface with and without Cross Flow. Report AD688953 von Karman Institute for Fluid Dynamics, Rhode-St., Genese, Belgium, Jan., 1969.
4. Abbott, W. A.: Studies of Flow Fields Created by Vertical and Inclined Jets when Stationary or Moving over a Horizontal Surface. ACR CP No. 911, 1967.
5. Schwantes, E.: The Recirculation Flow Field of a VTOL Lifting Engine, NASA TT F-14912, 1973.

6. Weber, H. A.; and Gay, A.: VTOL Reingestion Model Testing of Fountain Control and Wind Effects. Prediction Methods for V/STOL Propulsion Aerodynamics, vol. 1, Naval Air Systems Command, 1975, pp. 358-380.
7. Steger, J. L.; Ying, S. X.; and Schiff, L.B.: A Partially Flux-Split Algorithm for Numerical Simulation of Compressible Inviscid and Viscous Flow. Proceedings of a Workshop on Computational Fluid Dynamics held by the Institute of Nonlinear Sciences at the University of California at Davis, 1986.
8. Van Dalsem, W. R; and Steger, J. L.: The Fortified Navier-Stokes Approach. Proceedings of a Workshop on Computational Fluid Dynamics held by the Institute of Nonlinear Sciences at the University of California at Davis 1986.
9. Van Dalsem, W. R.; and Steger, J. L.: Using the Boundary-Layer Equations in Three-Dimensional Viscous Flow Simulation. Proceedings of the 58th Fluid Dynamics Panel Symposium on the Applications of Computational Fluid Dynamics in Aeronautics, paper 24, CP 412, Aix-en-Provence, France, 1986.
10. Steger, J. L.; and Van Dalsem, W. R.: Developments in the Simulation of Separated Flows Using Finite-Difference Methods. Proceedings of the Third Symposium on Numerical and Physical Aspects of Aerodynamic Flows, California State University, Long Beach, 1985.
11. Baldwin, B. S.; and Lomax, H.: Thin Layer Approximation and Algebraic Model for Separated Turbulent Flow. AIAA Paper No. 78-257, Jan., 1978.
12. Degani, D.; and Schiff, L. B.: Computation of Supersonic Viscous Flows Around Pointed Bodies at Large Incidence. AIAA Paper No. 83-0034, Jan., 1983.
13. Kuhn, R. E.; DelFrate, J. H.; and Eshleman, J. E.: Ground-Vortex Flow Field Investigation. Proceedings of the Ground-Vortex Workshop, NASA-Ames Research Center, April 22-23, 1987.
14. Taylor, G. I.: The Transport of Vorticity and Heat through Fluid in Turbulent Motion. Proc. Roy. Soc., vol. A., no. 135, pp. 685-703.
15. Smagorinsky, J.: General Circulation Experiments with the Primitive Equations, I, The Basic Experiment. Mon. Wea. Rev., vol. 91, pp. 99-165.
16. Rogallo, R. S.; and Moin, P.: Numerical Simulation of Turbulent Flows. Ann. Rev. Fluid Mech., vol. 16, 1984, pp. 99-137.
17. Childs, R. E.; and Nixon, D.: Unsteady Three-Dimensional Simulations of a VTOL Upwash Fountain. AIAA Paper No. 86-0212, Jan., 1986.
18. Rizk, M.; and Menon, S.: Large Eddy Numerical Simulation of an Array of Three-Dimensional Impinging Jets. Flow Research Report No. 403, May, 1987.
19. Billet, B.: Summary of an Experimental Investigation of the Ground Vortex. Proceedings of the Ground-Vortex Workshop, NASA-Ames Research Center, April 22-23, 1987.

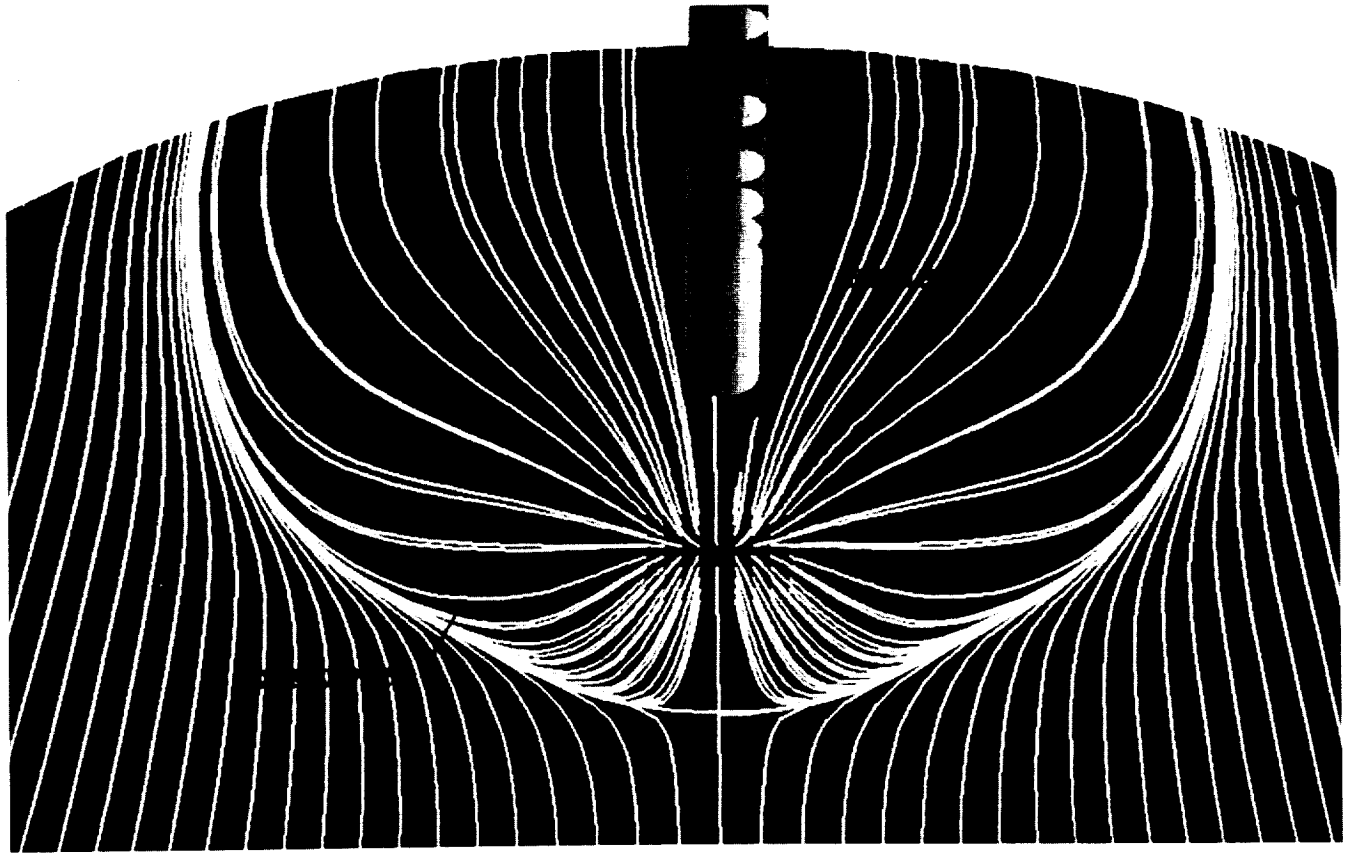

Figure 2.- Simulated oil-flow pattern showing jet footprint for a turbulent jet with $V_e = 0.223$ and $h/D = 3$ (front view).

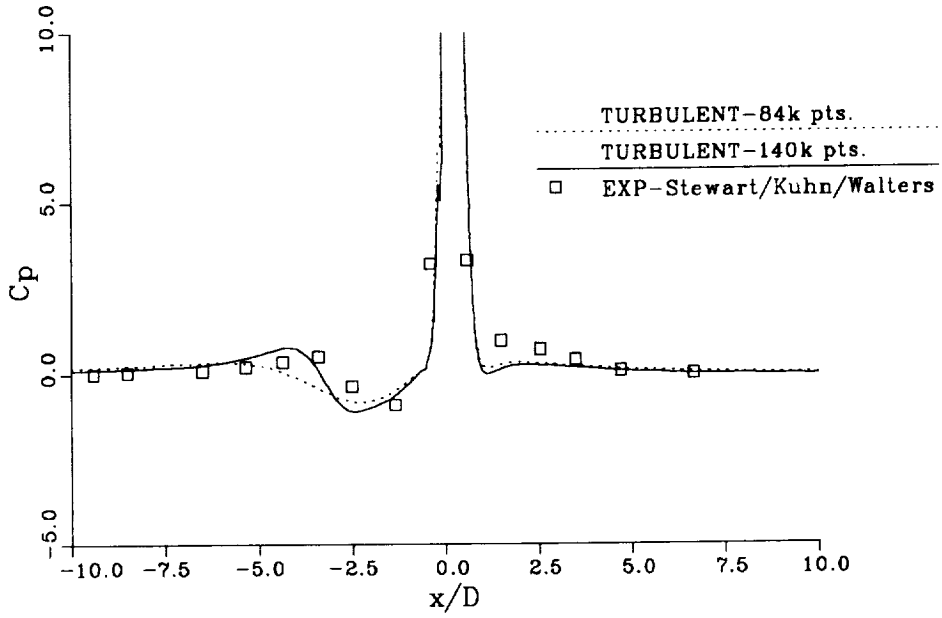

Figure 3a.- Impact of grid resolution on centerline C_p distributions for a turbulent jet with $V_e = 0.223$ and $h/D = 3$.

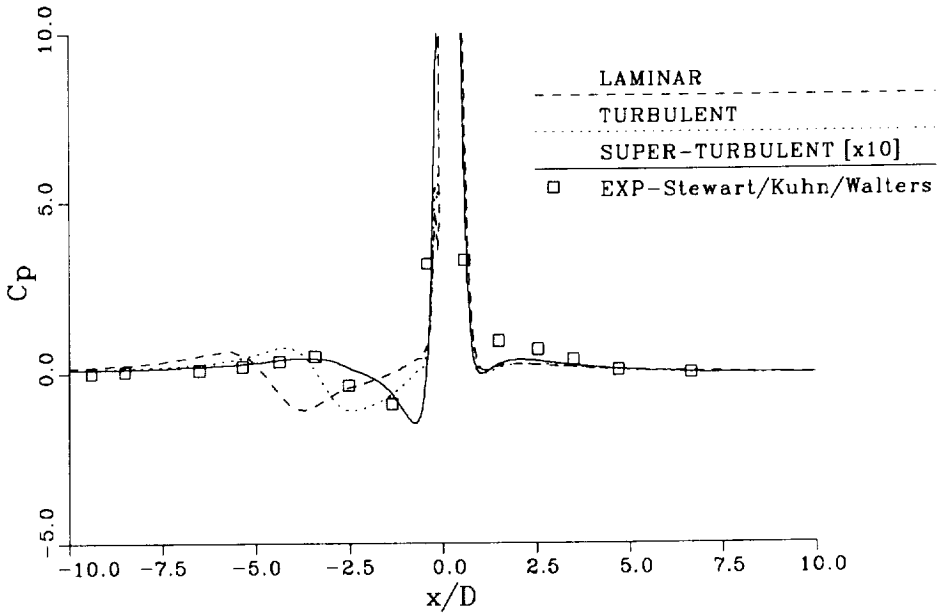

Figure 3b.- Impact of jet turbulence level on location of ground vortex, as shown by centerline C_p distributions for a jet with $V_e = 0.223$ and $h/D = 3$.

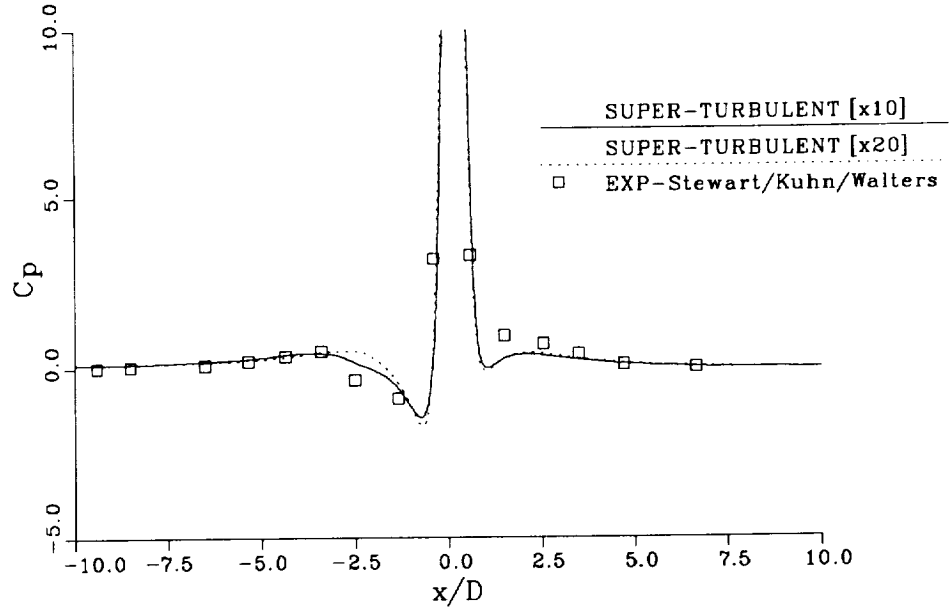

Figure 3c.- Relative insensitivity of centerline C_p distribution for a jet with $V_e = 0.223$ and $h/D = 3$ on jet turbulence level once a high turbulence level has been reached.

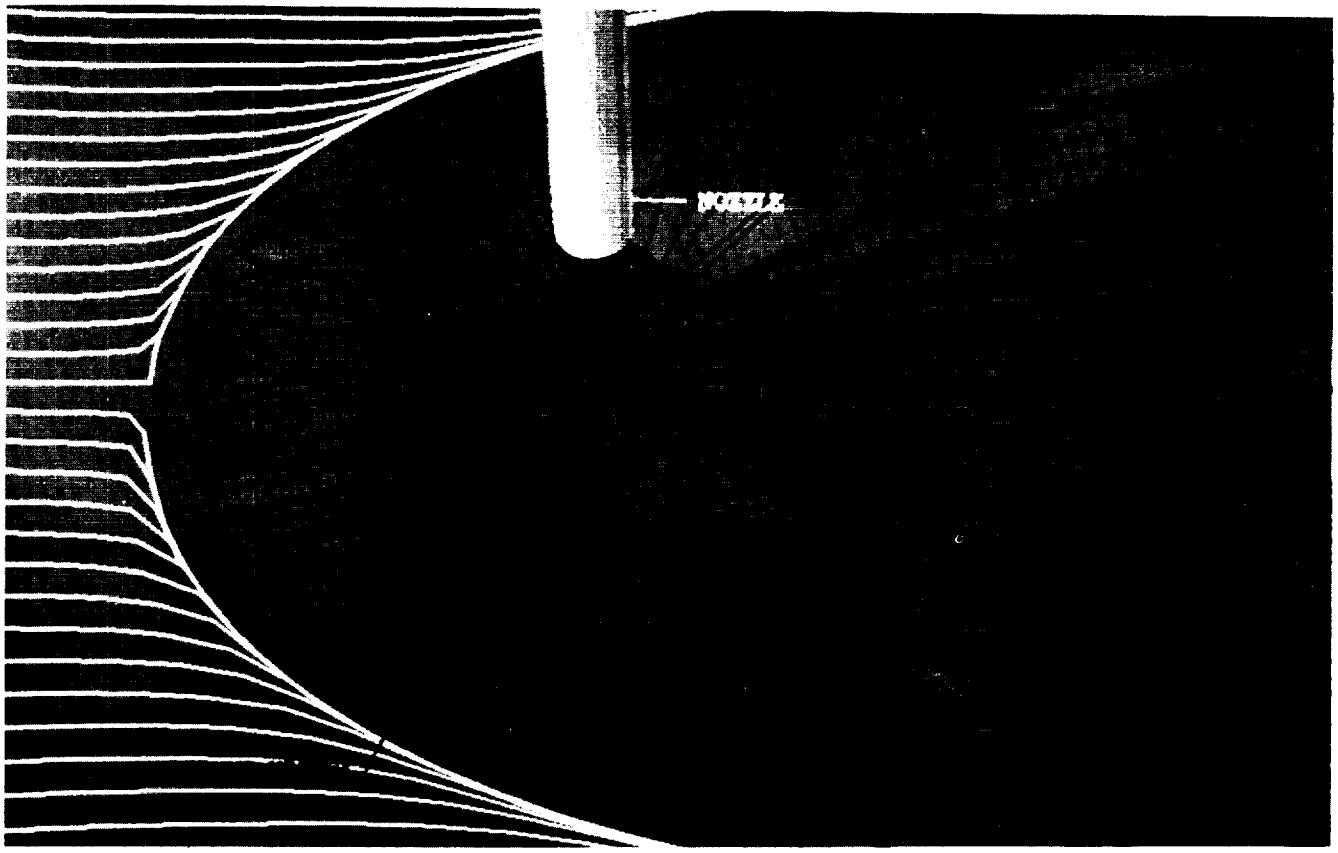

Figure 4a.- Particle traces for a laminar jet with $V_e = 0.223$ and $h/D = 3$ (top view).

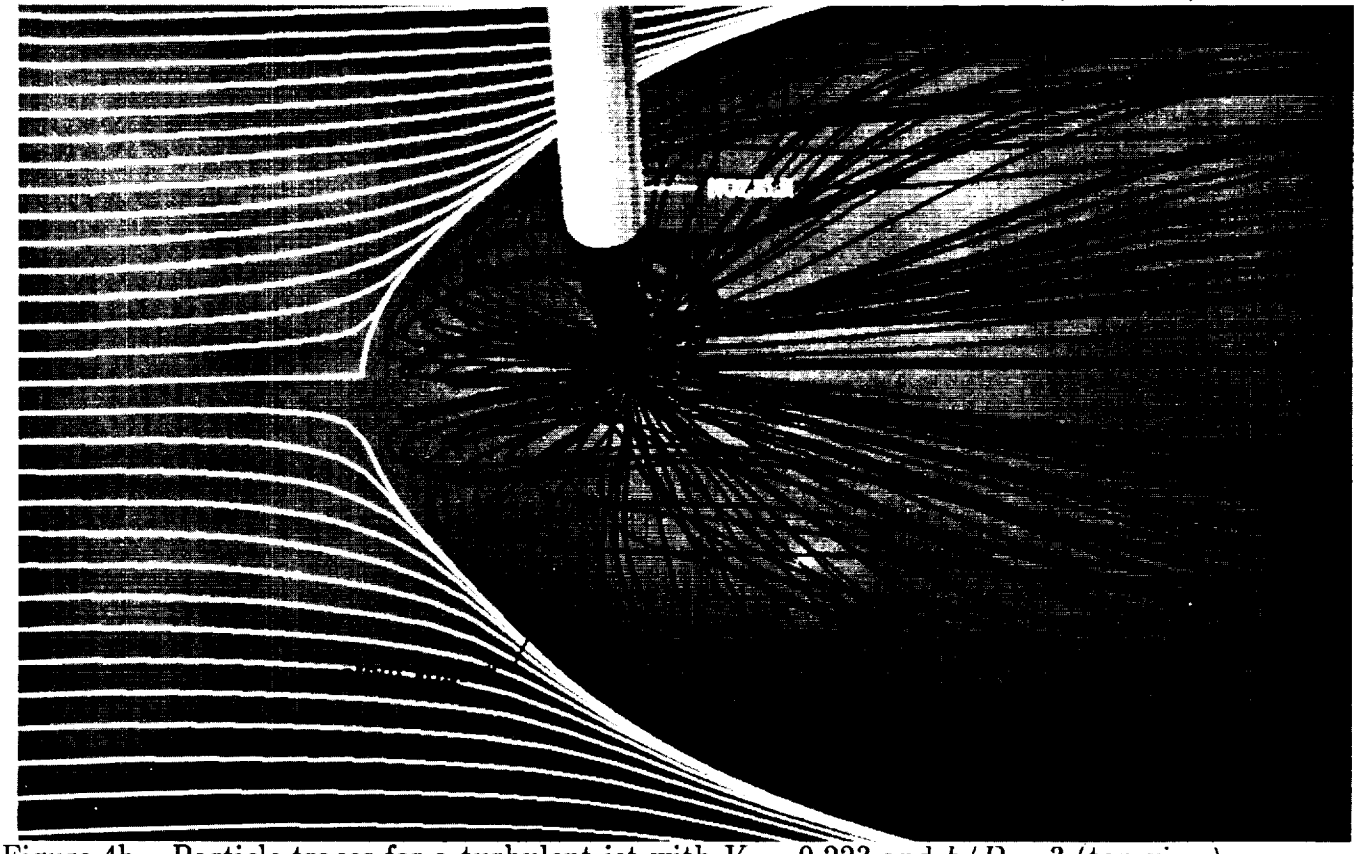

Figure 4b.- Particle traces for a turbulent jet with $V_e = 0.223$ and $h/D = 3$ (top view).

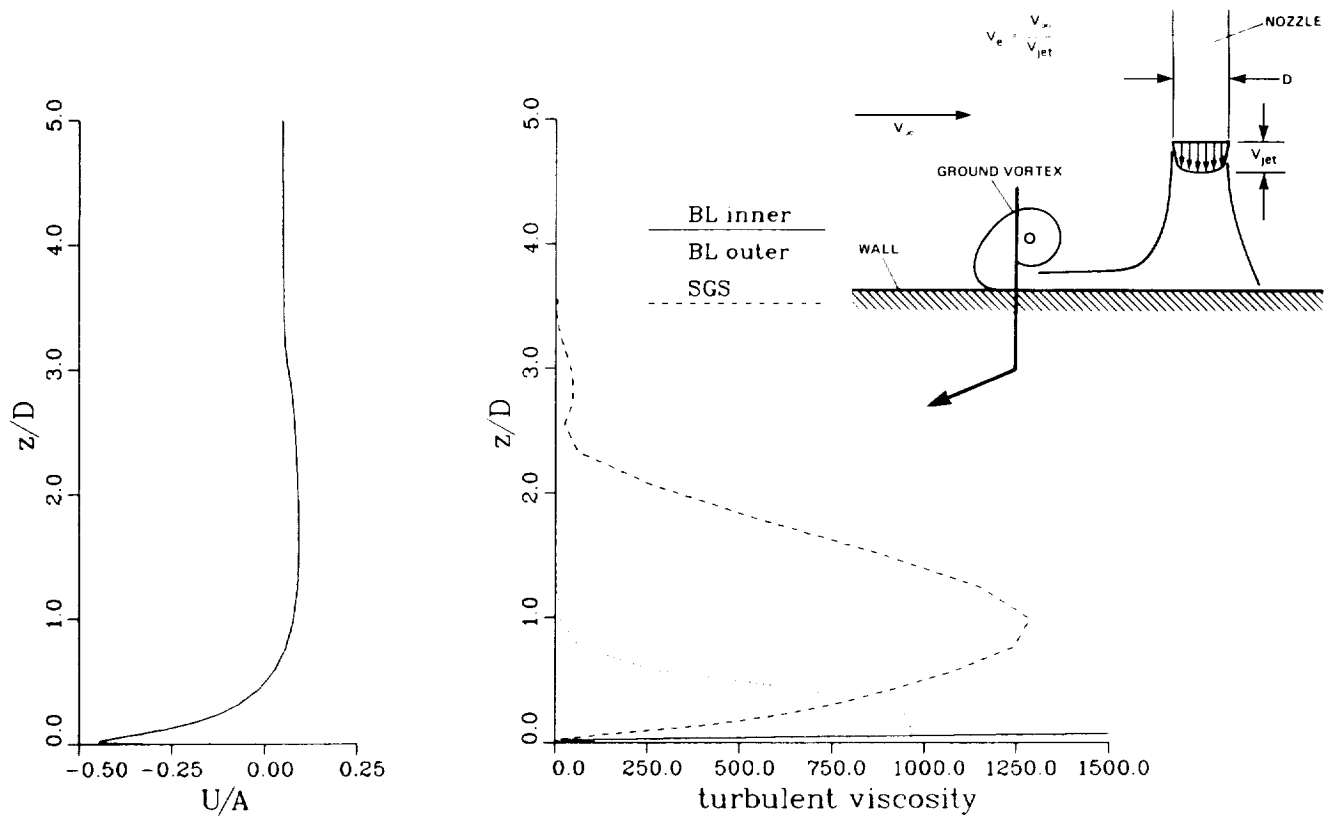

Figure 5a-b.- Streamwise velocity and turbulent viscosity (nondimensionalized by the molecular viscosity) profiles within the ground vortex.

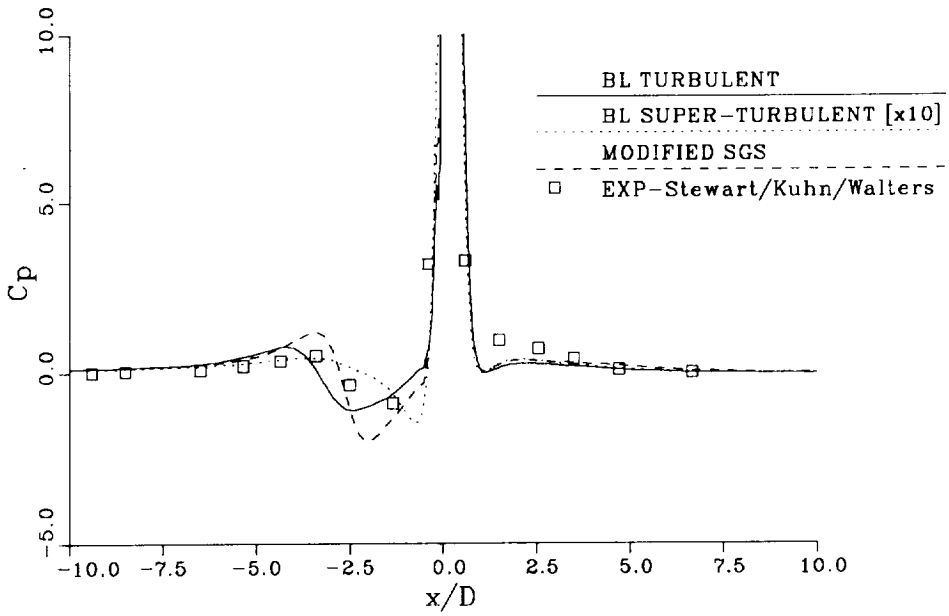

Figure 5c.- Impact of turbulence modeling on centerline C_p distribution for a jet with $V_e = 0.223$, and $h/D = 3$.

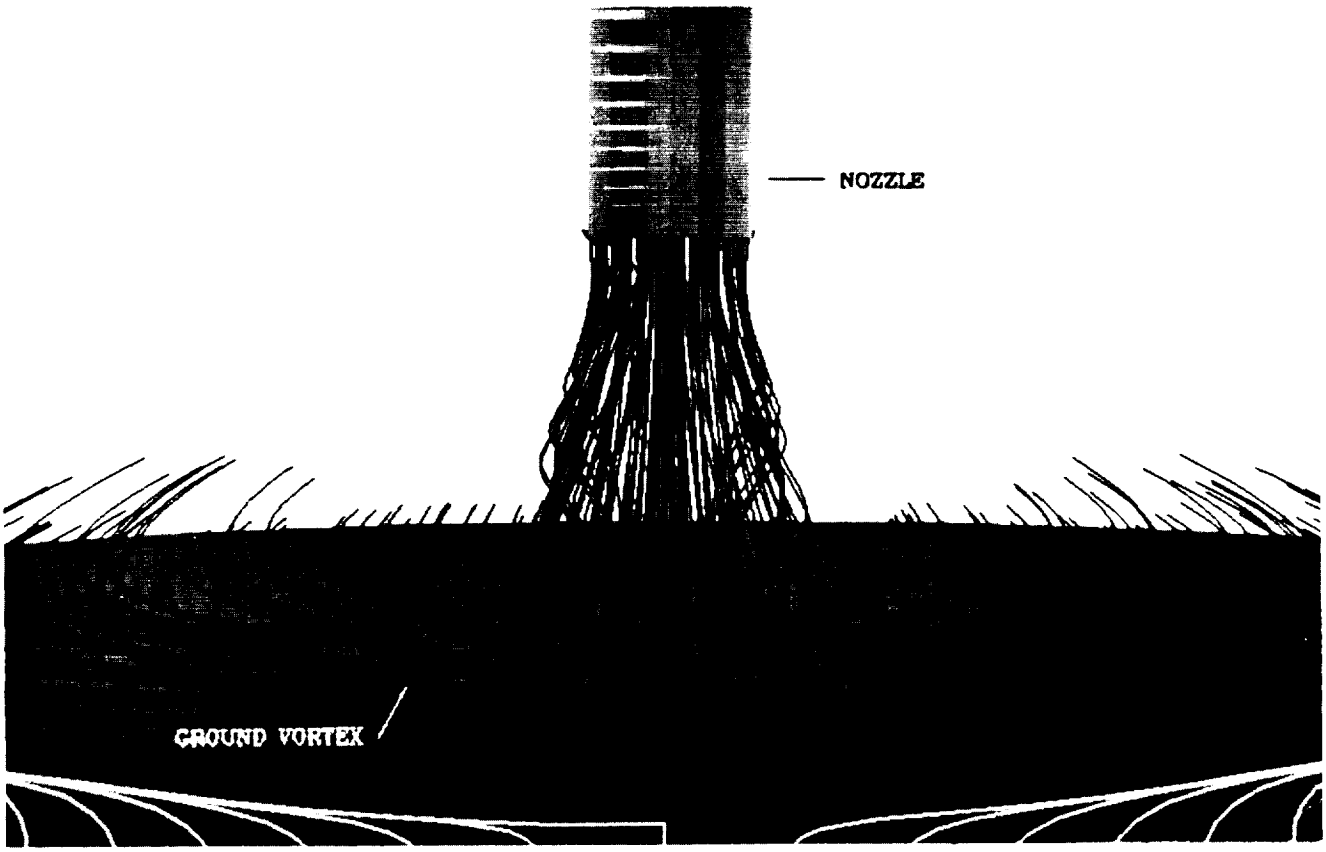

Figure 6.- Particle traces for a turbulent jet with $V_e = 0.223$ and $h/D = 3$ (front view).

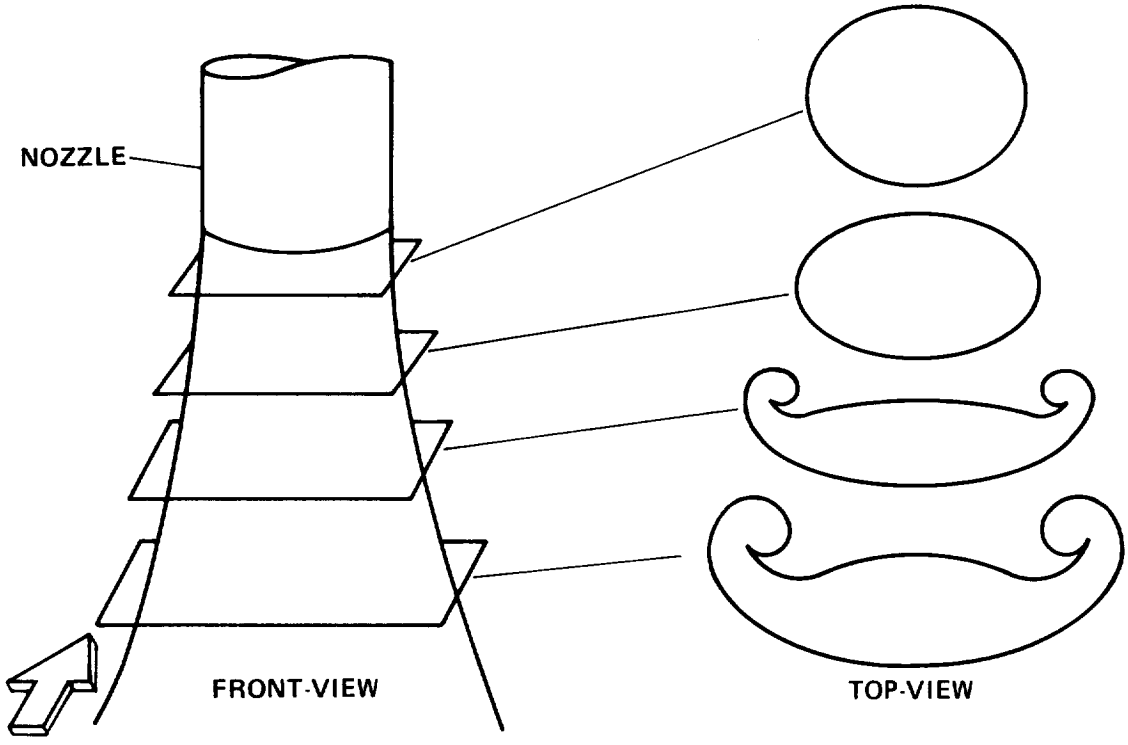

Figure 7.- Observed deformation of jet caused by pressures induced by freestream flow.

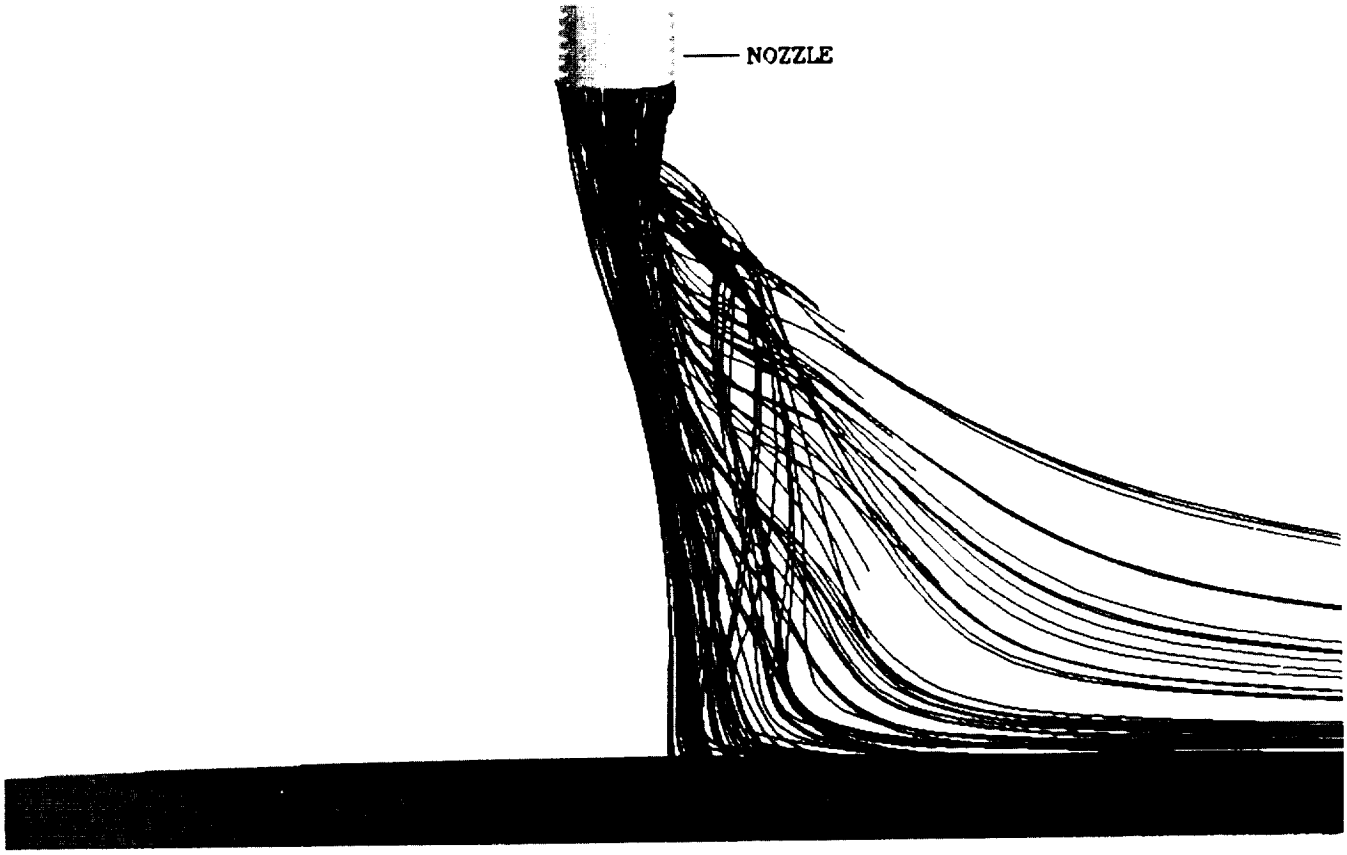

Figure 8.- Particle traces for a turbulent jet with $V_e = 0.223$ and $h/D = 6$ (side view).

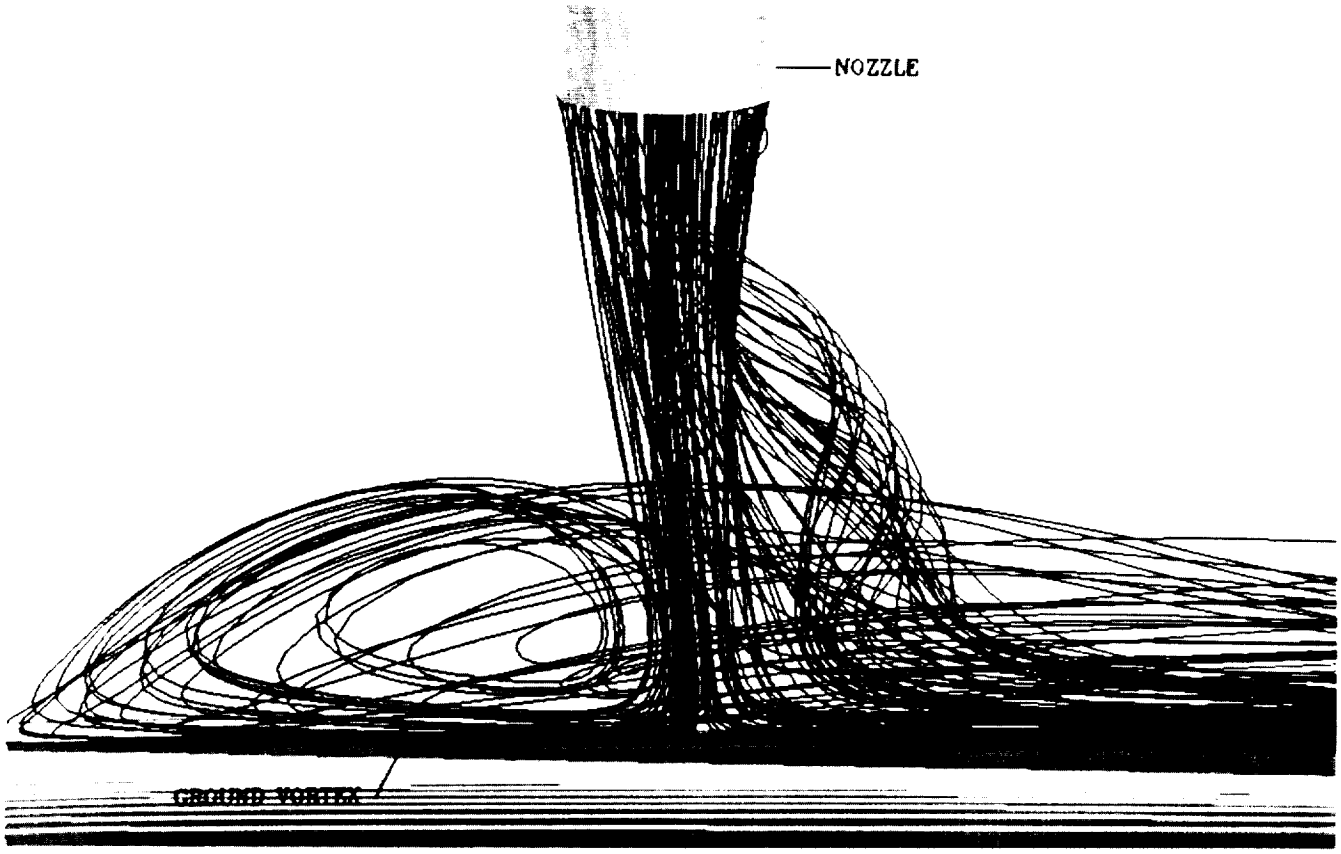

Figure 9a.- Particle traces for a turbulent jet exiting from a nozzle with $V_e = 0.223$ and $h/D = 3$ (side view).

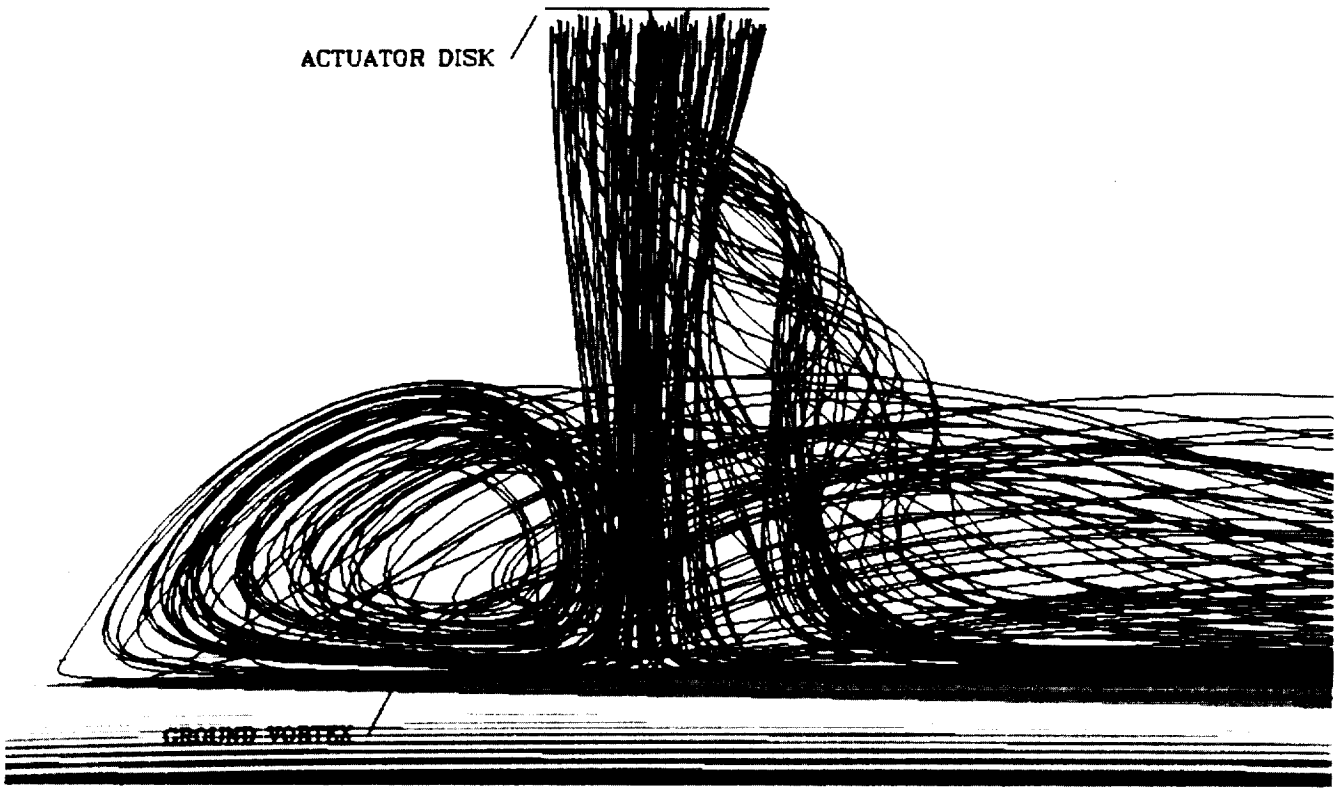

Figure 9b.- Particle traces for a turbulent jet exiting from an actuator disk with $V_e = 0.223$ and $h/D = 3$ (side view).

PANEL DISCUSSION

Summarized by R. E. Kuhn

The panel discussion took place on the morning of April 23, 1987. Mr. Richard J. Margason was moderator and the panelists were the speakers who presented the papers on the previous day. They were:

Vearl R. Stewart
Michael L. Billet
Richard E. Kuhn
William B. Blake
John W. Paulson, Jr.
A. Krothapalli
Paul T. Soderman
William R. Van Dalsem
Robert Childs

In addition to the panel members there were about 20 in the audience, many of whom took part in the discussion.

Prior to the discussion there were two presentations illustrating the broad nature of the ground vortex phenomena. Dr. Fred Schmitz presented a movie of the ground vortex generated by the downwash from a helicopter operating in ground effect. The problem being demonstrated concerned the loss of directional control encountered by the UH-1 helicopter hovering in a quartering tail wind. Under certain conditions the ground vortex could engulf the tail rotor and because the direction of rotation of the tail rotor and the ground vortex were the same tail rotor thrust would be decreased and directional control would be lost.

Mr. Margason showed slides illustrating the ground vortex type flow fields experienced by tilt wing, jet flap and jet V/STOL configurations in STOL operation and pointing out the lift loss, control problems and ingestion problems encountered under certain operating conditions. The presentations of the previous day had concentrated on the ground vortex flow fields generated by jet impingement, however these presentations showed that the phenomena was independent of disk loading and occurred at all scales.

The early part of the discussion concentrated on the fluid mechanics aspects of the flow field and the highly unsteady nature of the flow. Possible origins of the unsteadiness, the effects of noise, and the possibility of a feed back from the flow field on the ground to the flow exiting the nozzle were discussed. Much of the discussion was directed at what we need to know to provide a basis for successful CFD calculations. Significant progress is being made in developing CFD methods to calculate these types of flows and these efforts should be accelerated. Obtaining a clearer understanding of the physical mechanisms involved is key to the development of improved CFD methods.

It was clear that the vortices developed in the shear layer of an open jet issuing into free air, and the spreading of these vortices when the jet impinges on the ground play a role, and that under some conditions there is a feedback between the effects of these vortices and the turbulence of the jet. However the importance of the turbulence of the jet as it issues from the nozzles, relative to the turbulence generated by impingement and in the wall jet is not known. Nor is it clear that it is necessary to include feedback between the turbulence generated on the ground and the flow issuing form the nozzle to calculate the flow developed. Similarly it is clear that the impingement of the jet on the ground increases the noise of the jet but whether or not a feedback mechanism is necessary to explain this increase in noise or how it affects the development of the ground vortex flow field is unknown. The reduced forward projection of the ground vortex flow field with a moving ground plane (rather than a fixed ground board, as in conventional wind tunnel tests) has been shown but the extent to which this effect is due to the elimination of the free stream boundary layer, the additional scrubbing action of the ground moving aft under the wall jet or whether other mechanisms are also involved is not clear. Additional carefully structured tests, as well as CFD analysis, will be needed to answer all of these questions.

The effects of the ground vortex on the aerodynamics of an aircraft in ground effect was the next area discussed. Here it was pointed out that the different assumptions with regard to how the flow field develops and how it may be calculated may not be significant with respect to the effects on the aircraft. The data available demonstrates that, on a time averaged basis, the flow field is steady and its effects on the aircraft will be repeatable. What is needed with respect to the effects on the aircraft is the development of broadly based CFD methods for predicting the effects of the ground vortex flow field as well as a systematic data base to provide design guidelines and data for verification of the CFD methods. Carefully structured general research investigations are needed to develop this data base. In addition when tests of specific configurations are undertaken they should be structured to emphasize configuration build up so that the effects of the ground vortex on various components can be identified.

The ground vortex flow field is one of the mechanisms involved in the ingestion of hot gases and debris. Here the time averaged flow field will probably give a good indication of the average inlet temperature rise and thrust loss that may be encountered but not the temperature spikes which could cause surge. More work is needed to define the average flow field and resultant ingestion and also to define the extremes of the unsteadiness that will determine the operational limits for the configuration.

The third major area discussed was the effects of rate of descent on the development of the flow field and the resultant effects on the configuration. While it was pointed out that none of the many V/STOL test beds that have been flown have had any problems in landing that could be traced to the effects of rate of sink. It was also pointed out that most of these aircraft were depending primarily on the propulsion system rather than the wing for lift and

they did not include thrust reverser configurations which are subjected to a more intense ground vortex flow field. The need to develop equipment, similar to that already available in Europe, for wind tunnel investigations of the effect of rate of sink and rate of climb was identified. Also the need to keep the moving model facility at Langley operational until the more versatile wind tunnel equipment comes on line was stressed.

SUMMARY AND RECOMMENDATIONS

In summary the discussion identified 4 thrusts for future work on the ground vortex phenomena.

1. Basic fluid mechanics aspects: What is going on in the nozzle, the free jet, during impingement, in the wall jet, in the roll back caused by the free stream and in the free stream itself; what are the feed back mechanisms and how important are they; is noise a cause or effect; and what do we need to know to calculate the flow field. This will require the type of investigation conducted at Penn State and extensions to include the effects of controlled turbulence in the jet, measurements of the turbulence and space-time correlations of the unsteady pressures in the flow field and correlation with similar measurements on the flow fields generated by full scale jet engines.

2. Effects on the aircraft: The ground vortex can induce large lift losses, pitching moments and rolling moments on aircraft configurations. In addition it is one of the primary mechanisms in hot gas ingestion. The CFD methods for calculating the ground vortex flow field should be extended to predicting these effects on the aircraft. A systematic data base on the effects of jet arrangement, aircraft configuration variables, etc. needs to be developed to provide design guidelines as well as to provide data for validation of these CFD methods.

3. Effects of rate of descent and rate of climb: The work started in the moving model facility at Langley has shown that there are time dependent aspects to the development of the flow field and to the forces and moments experienced by configurations (particularly thrust reverser equipped configurations) entering ground effect. This work should be continued and equipment for making these types of investigations in wind tunnels should be developed. The moving model facility at Langley should be kept operational at least until comparable capability is developed for wind tunnel investigations.

4. Flight tests: Available aircraft (presently the QSRA and the YAV-8B Harrier) should be used to provide full scale flight data for verification of both wind tunnel data and computational methods. Flight test data should be reviewed and programs set up to obtain ground vortex flow field data as well as data on the effects of the ground vortex flow field on the aircraft. Related wind tunnel tests and computations should follow these flight programs so that the configurations, variables and operating conditions can be faithfully matched.

REFERENCES

During the discussion reports of several investigations pertinent to the ground vortex problem were mentioned. Each panelist was asked to supply citations of these and other references that illustrate and amplify the points made and provide additional information on the ground vortex problem. The following are the references supplied.

1. Binion, T. W. Jr.; "Investigation of the Recirculation Region of a Flow Field Caused by a Jet in Ground Effect With Crossflow". AEDC-TR-70-192, September 1970.

2. Childs, R. E., and Nixon, D.; "Unsteady Three-Dimensional Simulation of a VTOL Upwash Fountain". AIAA-86-0212, January 1986.

3. Childs, R. E., Nixon, D., Kuhn, G. D. and Perkins, S. C.; "Further Studies of Impinging Jet Phenomena". AIAA-87-0017, January 1987.

4. Ho, C. M. and Nossier, N. S.; "Dynamics of an Impinging Jet, Part 1: The Feedback Phenomenon". Journal of Fluid Mechanics, Vol. 105, 1981, pp. 119-142.

5. Nossier, N. S. and Ho, C. M.; "Dynamics of an Impinging Jet, Part 2: The Noise Generation". Journal of Fluid Mechanics, Col. 116, 1982, pp. 379-391.

6. Neuwerth, G.; "Flow Field and Noise Sources of Jet Impingement on Flaps and Ground Surfaces". AGARD CPP-308, 1981, pp. 13.1-13.7.

7. Marsh, H. A.; "Noise Measurements Around a Subsonic Air Jet Impinging on a Plane Ground Surface". Journal of Acoustical Society of America, Vol. 33, 1961, pp. 1065-1066.

8. Wagner, R. F.; "The Sound and Flow Field of an Axially Symmetric Free Jet Upon Impact on a Wall". NASA TTF-13942, 1971.

9. Krothapalli, A.; "Discrete Tones Generated by an Impinging Underexpanded Rectangular Jet". AIAA Journal, Vol. 23, No. 12, December 1985, pp. 1910-1915.